Front. Optoelectron. China 2011, 4(1): 59–64
DOI 10.1007/s12200-011-0205-2

RESEARCH ARTICLE

Dependence of porosity, charge recombination kinetics and photovoltaic performance on annealing condition of TiO_2 films

Chang-Ryul LEE, Hui-Seon KIM, Nam-Gyu PARK (✉)

School of Chemical Engineering, Department of Energy Science, Sungkyunkwan University, Suwon 440-746, Korea

Abstract Effect of annealing temperature, time of nanocrystalline TiO_2 film on porosity, electron transport/recombination and photovoltaic performance on dye-sensitized solar cell (DSSC) had been investigated in this article. Photocurrent density was slightly higher as annealing at 550°C compared to those of annealing at 450°C and 500°C under the given annealing time of 60 min, which was correlated with the amount of adsorbed dye. Thermogravimetric analysis showed there was a more weight loss between 500°C and 550°C, which revealed there were more sites for dye adsorption. Given the annealing temperature of 550°C, as annealing time varied from 60 to 90 and 120 min, results showed that the average size of pore and surface area decreased with longer annealing time, which deteriorated photocurrent density due to less dye loading. Electron diffusion rate remained almost unchanged regardless of annealing condition. However, electron recombination was influenced by annealing condition, it became slower with the increase of the annealing temperature under the given annealing time. In the contray, the electron recombination developed faster for the longer annealing time at a given annealing temperature. These results suggested that heat treatment of TiO_2 film at 550°C for 60 min in air would be the optimal annealing condition to achieve high efficiency DSSC.

Keywords dye-sensitized solar cell (DSSC), annealing conditions, surface area, porosity, electron life time

1 Introduction

Since the first report on dye-sensitized solar cell (DSSC) in 1991 [1], copious amounts of reports have been published to understand its working principle and to improve the solar-to-electrical conversion efficiency. The conversion efficiency as high as 11% has been achieved as a result of technological progress in DSSC [2–4]. The basic constituents of DSSC are dye, TiO_2 and redox electrolyte, where each plays a role in light absorption, electron transport and dye regeneration, respectively. Except for the role of electron transport in TiO_2, it acts as a support to adsorb dye molecules. Thus, TiO_2 is one of the most important constituents in DSSC. According to the results reported previously, morphology and porosity of TiO_2 film are critical to dye adsorption, electron transport and charge recombination [5–15]. Therefore, preparation procedure of TiO_2 film is of critical importance to overall conversion efficiency of DSSC.

There will be two important parameters affecting the TiO_2 film quality, annealing temperature and time. Nakade et al. [16] reported on the effect of annealing temperature of TiO_2 (S2 sample) on the photovoltaic performance in DSSC, where amount of adsorbed dye was slightly increased from 8.4×10^{-11} to 9.3×10^{-11} mol·cm^{-2} as the annealing temperature increased from 150°C to 450°C, however, the photocurrent density increased more than two times from 4.04 to 9.52 mA·cm^{-2}. Zhao et al. [17] reported that the adsorbed amount of dye decreased gradually with increasing the annealing temperature from 350°C to 600°C, while the photocurrent density increased from 350°C to 500°C, reached maximum at 500°C and decreased from 500°C to 600°C. For instance, the adsorbed dye concentration of 6.07×10^{-8} mol·cm^{-2} at 350°C decreased to 3.48×10^{-8} mol·cm^{-2} at 600°C, however, the photocurrent density increased from 2.87 to 9.84 mA·cm^{-2}. The reported results indicate that photovoltaic property is likely to be significantly influenced by annealing condition. Therefore, we have been motivated to investigate systematically the effect of annealing condition of TiO_2 film on photovoltaic performance. Here we report on

Received October 18, 2010; accepted December 30, 2010

E-mail: npark@skku.edu

effects of not only annealing temperature but also annealing time on TiO_2 film porosity, electron transport and recombination, and photovoltaic performance of DSSC.

2 Experiment

Fluorine-doped tin oxide (FTO) glasses (Pilkington, TEC-8, 8 Ω/sq, 2.3 mm thick) were cleaned with ethanol. FTO surface was pre-treated with Ti (IV) bis(ethylacetoacetato) diisopropoxide (Aldrich, 75%) solution, followed by heating at 500°C for 15 min. TiO_2 particles were hydrothermally synthesized using titanium isopropoxide (Aldrich, 97%) at 230°C for 12 h [18]. TiO_2 paste composed of TiO_2 particle, terpineol (Aldrich, 99.5%), ethyl cellulose (Aldrich, 46.000 cps) and lauric acid (Fluka, 96%) was coated on a FTO glass by doctor-blade method, which was annealed at different temperatures of 450°C, 500°C, and 550°C for 60 min. The annealing time at the given temperature was varied from 60 to 120 min.

Annealed TiO_2 films were sensitized with N719 dye (Esolar), where N719 stands for $Ru[LL'(NCS)_2]$, L = 2,2'-bypyridyl-4,4'-dicarboxylic acid, L' = 2,2'-bypyridyl-4,4'-ditetrabutylammonium carboxylate, for 9 h at 40°C. Pt counter electrode was prepared by spreading a 7 mM of H_2PtCl_6 in 2-propanol on a 1.5 cm × 2 cm sized FTO glass, which was heated at 400°C for 15 min in air. The dye-adsorbed TiO_2 electrode and the Pt counter electrode were sealed with 25 μm-thick Surlyn (Dupont 1702) at a pressure of 210 kPa·cm^{-2} and a temperature of about 100°C. The electrolyte used for this study was composed of 0.7 M 1-methyl-3-propyl-imidazolium iodide (MPII), 0.03 M I_2 (Aldrich, 99.8%), 0.05 M guanidinium thiocyanate (GuSCN) (Aldrich, 97%) and 0.5 M 4-*t*-butylpyridine (Aldrich, 96%) in acetonitrile (Fluka, 99.9%) and valeronitrile (Aldrich, 99.5%) (85∶15 *v*/*v*). The active area was measured by a digital microscope camera (DCMe 500) equipped an image-analysis program. TiO_2 film thickness was measured by Tencor alpha-step profiler.

Photocurrent and voltage were measured from a solar simulator equipped with 1000 W Xenon lamp (Newport 6271) and a Keithley 2400 source meter. Light intensity was adjusted with the NREL-calibrated Si solar cell having KG-2 filter for approximating one sun light intensity (100 mW·cm^{-2}). The cell was covered with an aperture mask to measure short-circuit photocurrent and open-circuit voltage accurately [19–21]. Incident-photon-to-current conversion efficiency (IPCE) was measured using a specially designed IPCE system for dye-sensitized solar cell (PV measurement, Inc.). A 75 W Xenon lamp was used as a light source for generating monochromatic beam. Calibration was accomplished using a silicon photodiode, which was calibrated using the NIST-calibrated photodiode G425 as a standard. IPCE data were collected at DC measurement mode with a chopping speed of 10 Hz. Thermogravimetric analysis of TiO_2 paste was performed at the rate of 5°C/min from ambient temperature to 600°C under N_2 stream by using a TG/DTA setup (SEICO Ins. 7300). Amount of the adsorbed dye was calculated from the absorbance at 510 nm obtained by Agilent 8453 UV-Vis spectrophotometer, where dye was desorbed by immersing the dye-covered TiO_2 films in a 10 mL of 0.1 M NaOH aqueous solution for 10 min. The morphology of TiO_2 films was investigated by scanning electron micrographs (SEM) (JSM-7500F JEOL). Surface area of TiO_2 particle was measured by Brunauer-Emmett-Teller (BET) setup (Micromertics Instrument Corp. ASAP 2020).

Time constants for photo-injected electron transport and recombination were measured by using a photocurrent and photovoltage transient setup. The cells were probed with a weak laser pulse at 532 nm superimposed on a relatively large, back ground (bias) illumination at 680 nm. The bias light was illuminated by a 0.5 W diode laser (B&W TEK Inc., Model: BWF1-670-300E/55370). The intensity of the bias light was adjusted using ND filters (neutral density filters). The 680 nm bias light is only weakly absorbed by the dye, and therefore the injected electrons are introduced into a narrow spatial region of the film, corresponding to where the probe light enters the film. A 30 mW frequency-doubled Nd:YAG laser (Laser-Export Co. Ltd. Model: LCS-DTL-314QT) (λ = 532 nm, pulse duration 10 ns) was used as probe light. The photocurrent transients were obtained by using a Stanford Research Systems model SR570 low-noise current preamplifier, amplified by a Stanford Research Systems model SR560 low-noise preamplifier, and recorded on Tektronics TDS 3054B digital phosphore oscilloscope 500 MHz 5GS/s DPO. The photovoltage transients were obtained by using SR560 preamplifier, which was recorded on oscilloscope combined with Keithley 2400 measure unit. The photocurrent- and the photovoltage-time curves were fitted with an exponential relationship, $y(t) = \exp(-t/\tau)$, where y represents photocurrent density or photovoltage, t is time and τ (τ_C for electron transport and τ_R for recombination) is constant.

3 Results and discussion

Temperature effect at a given annealing time and annealing time effect at a given temperature have been investigated: first, effect of annealing temperature on photovoltaic performance is investigated. Figure 1 compares photocurrent density of TiO_2 films annealed at 450°C, 500°C and 550°C for 60 min, along with the amount of adsorbed dye for each annealing temperature. Although there seems to be no significant difference in photocurrent density, the 550°C-annealed TiO_2 film shows relatively higher photocurrent density than those of 450°C and 500°C-annealed TiO_2 films. The amount of the adsorbed dye shows similar tendency. Thus, relatively higher photocurrent density for

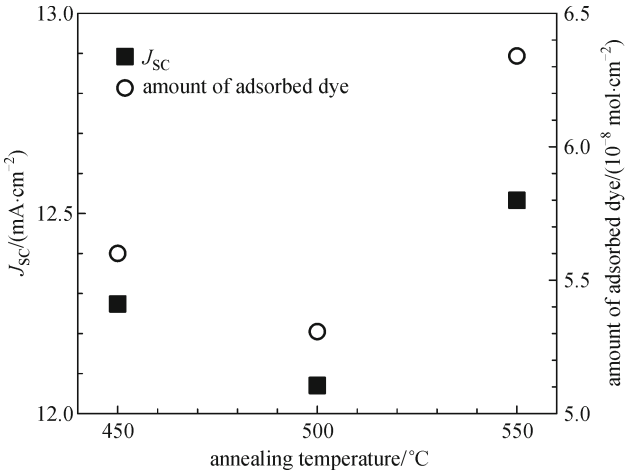

Fig. 1 Effect of annealing temperature on short-circuit photocurrent density (J_{SC}) and amount of adsorbed dye

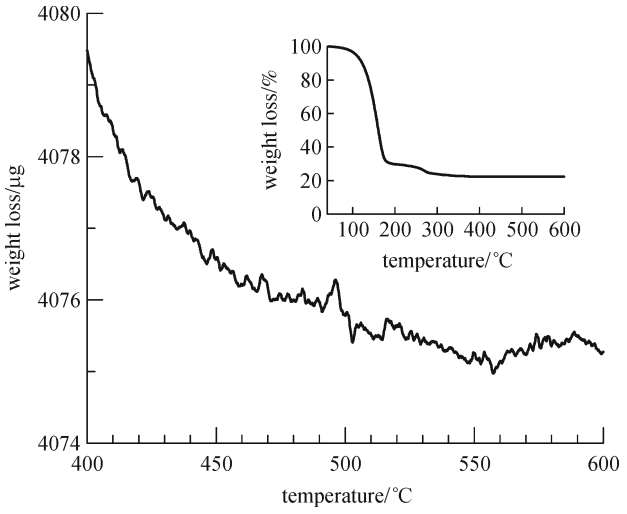

Fig. 2 Temperature-dependent weight loss of TiO_2 paste between 400°C and 600°C (thermal gravimetric analysis (TGA) curve in entire measured temperature range, and data were collected under N_2 atmosphere at a rate of 5°C/min)

the annealing temperature of 550°C is related to larger amount of the adsorbed dye. Photovoltaic parameters and amount of the adsorbed dye are listed in Table 1. Detailed thermogravimetric analysis in Fig. 2 confirms that a further weight loss is observed between 500°C and 550°C, which indicates that polymer binder in TiO_2 paste is not completely decomposed even at 500°C. Such a removal of the residual polymer binder at 550°C offers more sites for dye adsorption. No further change in weight loss is observed between 550°C and 600°C, indicating that decomposition of polymer binder is complete at 550°C. Since we have better performance with 550°C-annealed TiO_2 film, effect of annealing time is investigated at the fixed annealing temperature of 550°C.

Figures 3(a) and 3(b) show *I-V* curves and IPCE spectra for the different annealing times and the relevant photovoltaic parameters are summarized in Table 2. As annealing time increases from 60 to 90 min, photocurrent density decreases from 12.53 to 11.55 mA·cm^{-2}. The prolonged heat treatment upto 120 min shows photocurrent density of 11.63 mA·cm^{-2}, which means that photocurrent density seems to be little affected by annealing time longer than 90 min. IPCE data are well consistent with the observed photocurrent density. Measurement of amount of the adsorbed dye in Table 2 shows that the dye loading

Table 1 Short-circuit photocurrent density (J_{SC}), open-circuit voltage (V_{OC}), fill factor (*FF*), conversion efficiency (η) and amount of adsorbed dye for TiO_2 films annealed at different temperatures. Annealing temperature was varied at fixed time of 60 min. Measurements were performed under AM 1.5 G one sun light intensity (100 mW·cm^{-2}) and cell was covered with mask having aperture during measurement

annealing temperature	J_{SC}/(mA·cm^{-2})	V_{OC}/V	*FF*/%	η/%	amount of adsorbed dye/(10^{-8} mol·cm^{-2})	film thickness/μm
450°C	12.27±0.2	0.828±0.01	0.74±0.006	7.50±0.1	5.60	10.38
500°C	12.07±0.2	0.832±0.01	0.74±0.004	7.43±0.1	5.31	10.32
550°C	12.53±0.2	0.830±0.01	0.74±0.005	7.6±0.1	6.34	10.45

Table 2 J_{SC}, V_{OC}, *FF*, η, amount of adsorbed dye and surface area for TiO_2 films with different annealing times. Annealing time was varied at fixed temperature of 550°C. Measurements were performed under AM 1.5 G sun light intensity (100 mW·cm^{-2}) and cell was covered with mask having aperture during measurement

annealing time	J_{SC}/(mA·cm^{-2})	V_{OC}/V	*FF*	η/%	amount of adsorbed dye/(10^{-8} mol·cm^{-2})	film thickness /μm	surface area /(g·m^{-2})
60 min	12.53±0.2	0.830±0.01	73.37±0.5	7.67±0.1	6.34	10.40	65.62
90 min	11.55±0.3	0.836±0.01	72.95±0.5	7.05±0.1	5.87	10.22	47.99
120 min	11.63±0.1	0.824±0.01	71.70±0.9	6.83±0.1	4.39	10.37	44.70

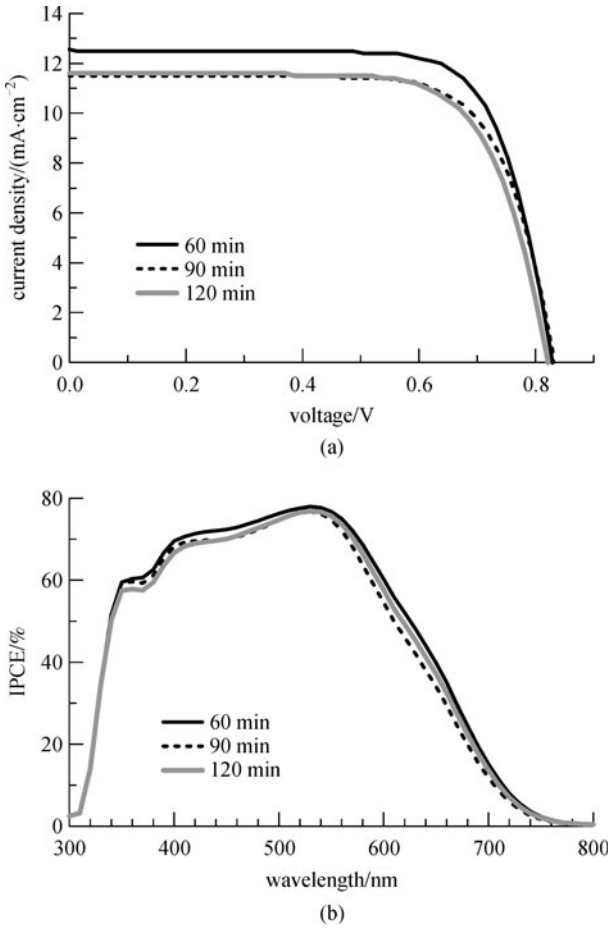

Fig. 3 (a) Photocurrent-voltage curves; (b) IPCE spectra of dye-sensitized solar cells with different annealing times of 60, 90, and 120 min at fixed temperature of 550°C

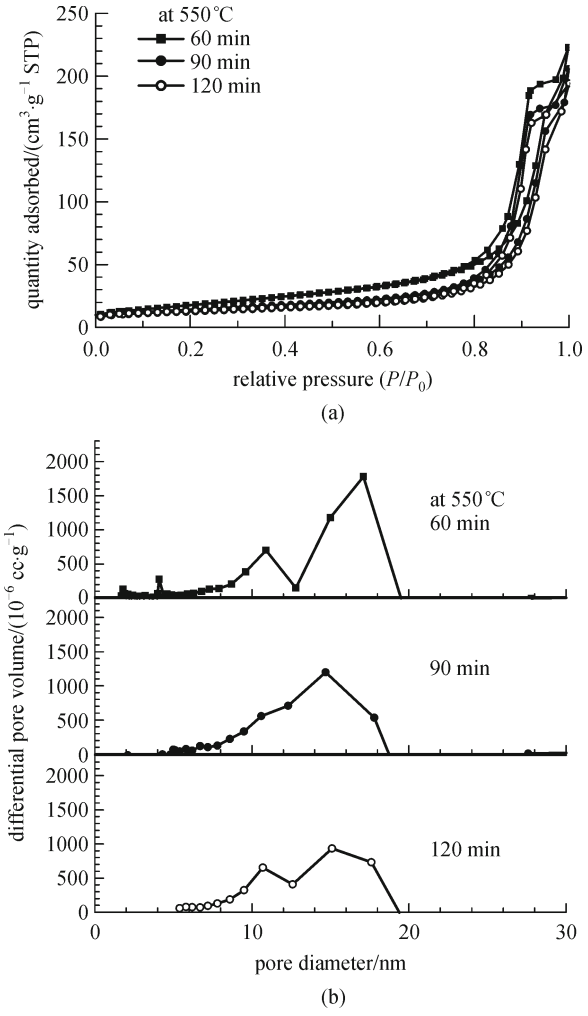

Fig. 4 Results of surface area measurement. (a) Nitrogen adsorption-desorption hysteresis loops; (b) pore distribution for TiO_2 films with different annealing time

quantity decreases with increasing the annealing time, which is responsible for the change in photocurrent density with annealing time. This observation implies that surface area may be changed with annealing time.

Figures 4(a) and 4(b) show the results of surface area measurement, where BET surface area is reduced from 66 to 48 and 45 $g \cdot m^{-2}$ as the annealing time increases from 60 to 90 and 120 min, respectively. Such a decrease in surface area is expected to change the average pore size. As can be seen from the pore size distribution in Fig. 4(b), 60 min-annealed TiO_2 film exhibits pore size with about 17 and 11 nm, where pore size of 17 nm is dominant. On the other hand, longer annealing time changes distribution of pore size, that is, the portion of 11 nm pores is larger, which indicates the average pore size is reduced. Decrease in photocurrent density as increasing the annealing time is therefore a consequence of the decreased surface area, associated with dye loading concentration.

In Figs. 5(a) and 5(b), SEM micrographs are compared for the TiO_2 films annealed for 60 and 120 min at fixed temperature of 550°C. TiO_2 particle aggregation is developed for the 120 min annealing time. This indicates that longer annealing time at 550°C induces fusion of particles, leading to decrease in average pore size and surface area as well, which is well consistent with the BET results in Fig. 4.

Figures 6(a) and 6(b) show time constants for electron recombination as a function of light intensity, represented by photocurrent density. Time constant is similar for both 450°C and 500°C, while it increases for the case of 550°C (Fig. 6(a)). This indicates that electron life time becomes longer as annealing temperature increases. Similar observation was reported previously for the annealing temperatures of 150°C and 450°C [16]. Mori et al. [22] also reported that the electron life time of the TiO_2 particles sintered at 450°C showed longer than that of the nonsintered one. It was interpreted that more traps lead to longer electron life time. Sintered TiO_2 particles would have more traps because of lower resistance at particle boundary due to better interparticle connection. For the

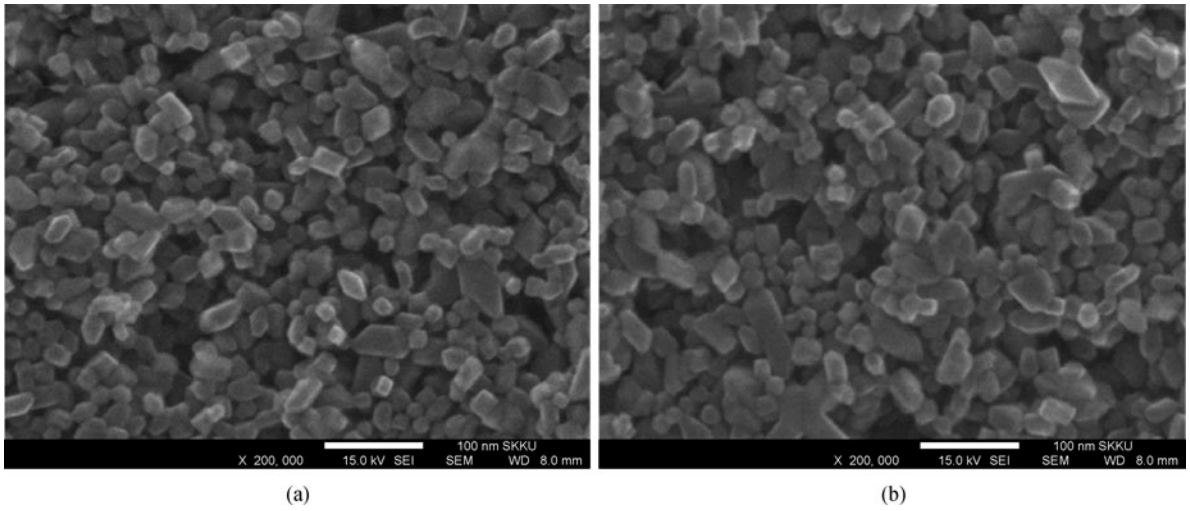

Fig. 5 SEM of TiO_2 nanoparticles with different annealing time at fixed annealing temperature of 550°C. (a) 60 min; (b) 120 min

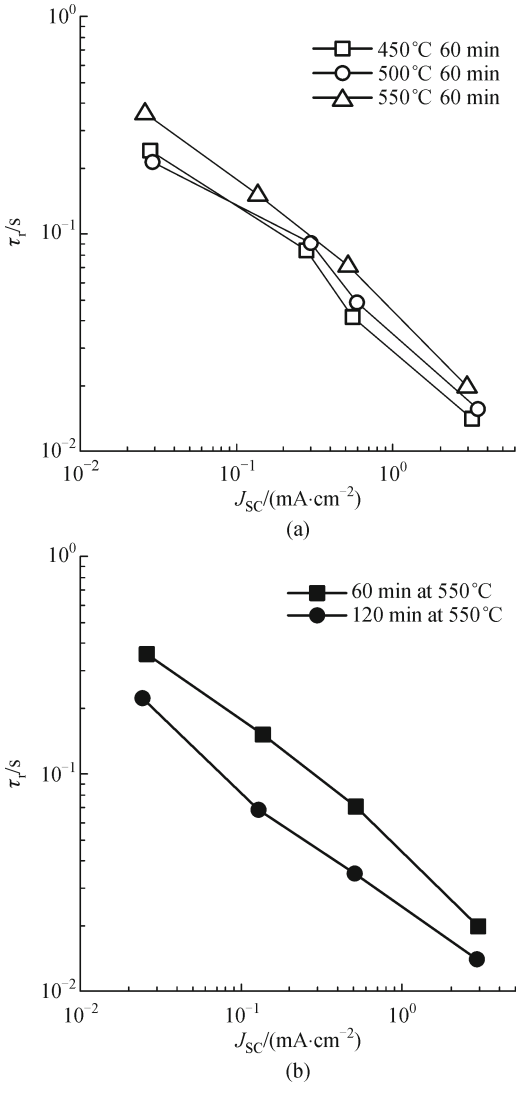

Fig. 6 Effect of (a) annealing temperature and; (b) annealing time on time constants for recombination

case of change in annealing time at fixed temperature, longer annealing time results in faster recombination as can be seen in Fig. 6(b). Nakade et al. [9] reported that larger sized TiO_2 particle showed shorter electron life time than the smaller sized one. Enlargement effect is induced by annealing for long time since longer annealing time decreases porosity and surface area. If we consider point contact among particles, number of point contact will be less for larger particle than for smaller one. Thus, the larger particle may have fewer traps, which leads to shorter electron life time. Regarding electron transport rate as a function of light intensity (not shown here), it is observed that change in the annealing condition has little influence on electron diffusion rate.

4 Conclusions

From the systematic investigation on effects of annealing temperature and time on photovoltaic property in DSSC, we drew conclusions as follows. Decomposition of ethyl cellulose used as a binder in TiO_2 paste was found to be completed at around 550°C. At the given temperature of 550°C, photovoltaic performance, especially photocurrent density, deteriorated under prolonged annealing. The annealing time longer than 60 min, such as 90 and 120 min, decreased surface area and porosity, resulting in the decrease of amount of adsorbed dye and, as a result, low photocurrent density. Change in annealing condition had little effect on electron transport at short circuit condition, while it affected significantly electron life time at open circuit condition. With the TiO_2 paste comprising 20 nm-sized anatase TiO_2 particles, ethyl cellulose polymer binder, lauric acid and terpineol, best photovoltaic performance can be obtained from the annealing of TiO_2 paste at the temperature of 550°C for 60 min.

Acknowledgements This work was supported by the National Research Foundation of Korea grant funded by the Ministry of Education, Science and Technology of Korea (No. 2010-0014992), R31-2008-000-10029-0 (WCU Program), and the Korea Institute of Energy Technology Evaluation and Planning grant funded by the Ministry of Knowledge Economy (No. 20103020010010).

References

1. O'Regan B, Grätzel M. A low-cost, high-efficiency solar cell based on dye-sensitized colloidal TiO_2 films. Nature, 1991, 353(6346): 737–740
2. Grätzel M. Dye-sensitized solar cells. Journal of Photochemistry and Photobiology C, Photochemistry Reviews, 2003, 4(2): 145–153
3. Grätzel M. Conversion of sunlight to electric power by nanocrystalline dye-sensitized solar cells. Journal of Photochemistry and Photobiology A Chemistry, 2004, 164(1–3): 3–14
4. Lee K T, Park S W, Ko M J, Kim K, Park N G. Selective positioning of organic dyes in a mesoporous inorganic oxide film. Nature Materials, 2009, 8(8): 665–671
5. Opara K U, Berginc M, Hocevar M, Topic M. Unique TiO_2 paste for high efficiency dye-sensitized solar cells. Solar Energy Materials and Solar Cells, 2009, 93(3): 379–381
6. Kavan L, Grätzel M, Rathousky J, Zukal A J. Nanocrystalline TiO_2 (anatase) electrodes: Surface morphology, adsorption, and electrochemical properties. Journal of the Electrochemical Society, 1996, 143(2): 394–400
7. Park N G, van de Lagemaat J, Frank A J. comparison of dye-sensitized rutile-and anatase-based TiO_2 solar cells. Journal of Physical Chemistry B, 2000, 104(38): 8989–8994
8. Adachi M, Jiu J, Isoda S. Synthesis of morphology-controlled titania nanocrystals and application for dye-sensitized solar cells. Current Nanoscience, 2007, 3(4): 285–295
9. Nakade S, Saito Y, Kubo W, Kitamura T, Wada Y, Yanagida S. Influence of TiO_2 nanoparticle size on electron diffusion and recombination in dye-sensitized TiO_2 solar cells. Journal of Physical Chemistry B, 2003, 107(33): 8607–8611
10. Zhu K, Kopidakis N, Neale N R, van de Lagemaat J, Frank A J. Influence of surface area on charge transport and recombination in dye-sensitized TiO_2 solar cells. Journal of Physical Chemistry B, 2006, 110(50): 25174–25180
11. Lee K M, Suryanarayanan V, Ho K C. A study on the electron transport properties of TiO_2 electrodes in dye-sensitized solar cells. Solar Energy Materials and Solar Cells, 2007, 91(15–16): 1416–1420
12. Centi G, Perathoner S. The role of nanostructure in improving the performance of electrodes for energy storage and conversion. European Journal of Inorganic Chemistry, 2009, 2009(26): 3851–3878
13. Cass M J, Qiu F L, Walker A B, Fisher A C, Peter L M. Influence of grain morphology on electron transport in dye sensitized nanocrystalline solar cells. Journal of Physical Chemistry B, 2003, 107(1): 113–119
14. van de Lagemaat J, Benkstein K D, Frank A J. Relation between particle coordination number and porosity in nanoparticle films: Implications to dye-sensitized solar cells. Journal of Physical Chemistry B, 2001, 105(50): 12433–12436
15. Aduda B O, Ravirajan P, Choy K L, Nelson J. Effect of morphology on electron drift mobility in porous TiO_2. International Journal of Photoenergy, 2004, 6(3): 141–147
16. Nakade S, Matsuda M, Kambe S, Saito Y, Kitamura T, Sakata T, Wada Y, Mori H, Yanagida S. Dependence of TiO_2 nanoparticle preparation methods and annealing temperature on the efficiency of dye-sensitized solar cells. Journal of Physical Chemistry B, 2002, 106(39): 10004–10010
17. Zhao D, Peng T Y, Lu S L, Cai P, Jiang P, Bian Z Q. Effect of annealing temperature on the phothelectrochemical properties of dye-sensitized solar cells made with mesoporous TiO_2 nanoparticles. Journal of Physical Chemistry C, 2008, 112(22): 8486–8494
18. Koo H J, Park J, Yoo B, Yoo K, Kim K, Park N G. Size-dependent scattering efficiency in dye-sensitized solar cell. Inorganica Chimica Acta, 2008, 361(3): 677–683
19. Koide N, Han L. Measuring methods of cell performance of dye-sensitized solar cells. Review of Scientific Instruments, 2004, 75(9): 2828–2831
20. Ito S, Nazeeruddin Md K, Liska P, Comte P, Charvet R, Pechy P, Jirousek M, Kay A, Zakeeruddin S M, Grätzel M. Photovoltaic characterization of dye-sensitized solar cells: effect of device masking on conversion efficiency. Progress in Photovoltaics: Research and Applications, 2006, 14(7): 589–601
21. Park J, Koo H J, Yoo B, Yoo K, Kim K, Choi W, Park N G. On the *I-V* measurement of dye-sensitized solar cell: Effect of cell geometry on photovoltaic parameters. Solar Energy Materials and Solar Cells, 2007, 91(18): 1749–1754
22. Mori S, Sunahara K, Fukai Y, Kanzaki T, Wada Y, Yanagida S. Electron transport and recombination in dye-sensitized TiO_2 solar cells fabricated without sintering process. Journal of Physical Chemistry C, 2008, 112(51): 20505–20509